© 2017. Published by The Company of Biologists Ltd | Journal of Experimental Biology (2017) 220, 469-477 doi:10.1242/jeb.144089

RESEARCH ARTICLE

Intramolecular interactions that control voltage sensitivity in the jShak1 potassium channel from *Polyorchis penicillatus*

Nazlee Sharmin[1,2] and Warren J. Gallin[1,*]

ABSTRACT

Voltage-gated potassium ion (Kv) channel proteins respond to changes in membrane potential by changing the probability of K^+ flux through an ion-selective pore. Kv channels from different paralogous and orthologous families have widely varying V_{50} values. The voltage-sensing transmembrane helices (S4) of different channels contain four to seven basic residues that are responsible for transducing changes in transmembrane potential into the energy required to shift the equilibrium between the open- and closed-channel conformations. These residues also form electrostatic interaction networks with acidic residues in the S2 and S3 helices that stabilize the open and the closed states to different extents. The length and composition of the extracellular loop connecting the S3 and S4 helices (S3–S4 loop) also shape the voltage response. We describe mutagenesis experiments on the jellyfish (*Polyorchis penicillatus*) Kv1 family jShak1 channel to evaluate how variants of the S3–S4 loop affect the voltage sensitivity of this channel. In combination with changes in the length and composition of the S3–S4 linker, we mutated a residue on the S2 helix (N227) that in most Kv1 family channels is glutamate (E226 in mouse Kv1.2, E283 in *D. melanogaster* Shaker). Some individual loop replacement mutants cause major changes in voltage sensitivity, depending on a combination of length and composition. Pairwise combinations of the loop mutations and the S2 mutations interact to yield quantitatively distinct, non-additive changes in voltage sensitivity. We conclude that the S3–S4 loop interacts energetically with the residue at position N227 during the transitions between open and closed states of the channel.

KEY WORDS: Allostery, Cnidaria, Ion channel, Structure–function

INTRODUCTION

The voltage-gated potassium ion (Kv) channels are transmembrane protein tetramers, consisting of a pore domain (PD), surrounded by four voltage-sensing domains (VSDs) (Lee et al., 2005; Tombola et al., 2006). The single PD consists of helices S5 and S6 and their connecting loops (P loops) from each subunit. The four distinct VSDs, in contrast, are each composed of helices S1 to S4 and their connecting loops from a single subunit. Depending on the channel, S4, the voltage-sensing helix, contains four to seven positively charged amino acid residues. Changes in membrane potential change the force acting on the charged residues of the S4 helix. This variation in force leads to changes in the probability of transition between the open and closed state protein conformations (Fig. 1) (Lee et al., 2005; Long et al., 2005). In most Kv1 family channels, three conserved negatively charged residues in the S2 and S3 helices interact with the conserved positively charged residues of the S4 helix to stabilize the open and the closed states of the channel (Lee et al., 2005; Long et al., 2005; Papazian et al., 1995). In the *Drosophila melanogaster* Shaker channel, the open conformation is stabilized by salt-bridges formed between R368 and R371 of the S4 helix and E283 of the S2 helix (Papazian et al., 1995; Silverman et al., 2003). The closed conformation is stabilized by salt bridges that are formed between K374 in the S4 helix and E293 and D316 in the S2 and S3 helices, respectively (Durell et al., 2004; Li-Smerin et al., 2000; Papazian et al., 1995; Tiwari-Woodruff et al., 1997). Although the charged residues of the VSD are conserved in most Kv channels, V_{50}, the membrane voltage at which 50% of the channels are in the open state, varies among and within the families of Kv channels in different species, indicating contributions of other factors in determining voltage sensitivity in different members of this channel family.

Previous studies with mouse Kv1.2 (Sand et al., 2013) and *D. melanogaster* Shaker (Gonzalez et al., 2001; Priest et al., 2013) indicated a role for the S3–S4 loop length and composition in setting the V_{50} of activation of the channel. The results of a mouse Kv1.2 study (Sand et al., 2013) demonstrate an energetic constraint in the movement of the S4 helix by extremely short S3–S4 linkers. Depending on composition, the C-terminal end of the mouse S3–S4 linker also differentially affected the equilibrium between open and closed states of the channel by interacting with the negatively charged turret of the pore domain (Sand et al., 2013), as this part of the P loop is positioned in close proximity to the negatively charged residues of VSD during channel closure (Jensen et al., 2012). In *D. melanogaster*, mutations that shorten the S3–S4 linker tend to shift the V_{50} to more positive values and decrease the rate of channel activation (Priest et al., 2013).

Here, we analyzed the effect of the S3–S4 linker variation on the voltage sensitivity of jShak1, a Kv1 family member from the jellyfish *Polyorchis penicillatus*. jShak1 differs from most other Kv1 channels in several important ways. jShak1 opens at a much higher membrane potential (V_{50}=+33.0 mV) than mouse Kv1.2 (V_{50}=−13 mV) or fruit fly Shaker (V_{50}=−32 mV). In jShak1, the homologous position of a conserved acidic residue of the S2 helix (E283 in *D. melanogaster* Shaker and E226 in mouse Kv1.2) is occupied by neutral asparagine, N227. Also, jShak1 has one less positively charged motif in the S4 region and a very short S3–S4 linker, consisting of only five amino acid residues (Grigoriev et al., 1997; Klassen et al., 2008), compared with any of the well-studied Kv1 family channels; the rat Kv1.2 S3–S4 loop consists of 18 amino acids, the *D. melanogaster* Shaker S3–S4 loop consists of 29 amino acids, and evaluation of 239 aligned Kv1 family channels finds a range of S3–S4 loop lengths between 5 and 30 amino acids, with a

[1]Department of Biological Sciences, University of Alberta, Edmonton, AB, Canada T6G 2E9. [2]Montreal Heart Institute, 5000 Belanger St Est, Montreal, QC, Canada T6G 2E9.

*Author for correspondence (wgallin@ualberta.ca)

W.J.G., 0000-0002-9937-3880

Received 31 May 2016; Accepted 17 November 2016

Journal of Experimental Biology (2017) 220, 469-477 doi:10.1242/jeb.144089

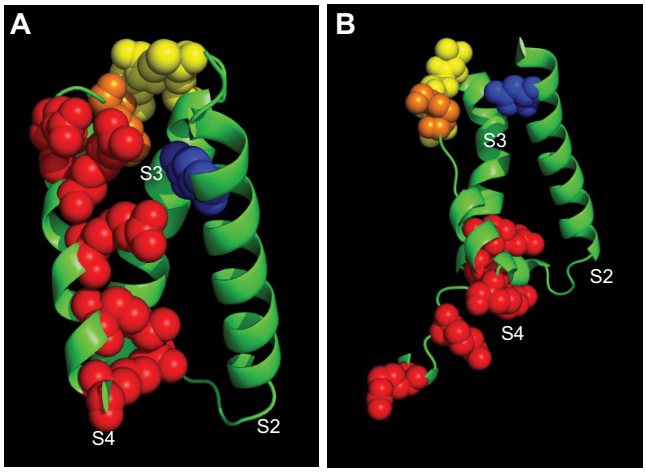

Fig. 1. Illustration of the spatial relationship between the relevant amino acid residues in the jShak1 channel in this study. (A) Open state and (B) closed state. The S2, S3 and S4 helices are shown, with the rest of the channel protein removed for clarity. The N residue at position 227 is shown as a blue space-filling model, the VSSSK S3–S4 loop residues are shown as yellow–orange space-filling models, with the C-terminal K278 residue in orange, and the basic, positively charged residues in the S4 helix are shown as red space-filling models. The remainder of the visible protein is illustrated in a cartoon format to show the arrangement of the backbone of this part of the channel.

mean value of approximately 17 amino acids. Mutations of the length of the S4 helix in conjunction with mutation of N227 in jShak1 indicated that the movement of the S4 helix might be constrained by the extremely short S3–S4 linker of the jShak1 channel (Klassen et al., 2008), in particular holding the S4 helix very close to the S2 helix in the open state.

The results of this study show that the effects of mutations that vary loop length and sequence on *P. penicillatus* jShak1 are substantially different from the effects of comparable mutations on mouse Kv1.2 channels (Sand et al., 2013). The length of these loops affects the voltage sensitivity of the channel, at least in part by constraining the relative movement of the S3 and S4 helices. The magnitude of the effect of a loop also varies depending on the identity of amino acid residues in the loop and at other sites in the protein, indicating that the loop interacts non-covalently with other parts of the channel protein, as part of a network of interactions that differentially stabilizes the open and closed state conformations of the channel. Combining the S3–S4 loop mutations with mutations to the N227 residue demonstrates that the effect of the loop mutations can be substantially different, both quantitatively and qualitatively, in the context of different residues at position 227.

MATERIALS AND METHODS

Mutant construction

To construct the jellyfish channel jShak1 (GenBank accession no. U32922) S3–S4 loop mutants, the non-inactivating (Δ23N) channel in pXT7 (Klassen et al., 2008) was used to create a construction vector with *Bsr*GI and *Bcl*I cutting sites at the S3–S4 loop margins, using overlapping PCR (Ho et al., 1989). To make the loop mutants, synthetic oligonucleotides were designed with the desired loop sequence and overhangs of *Bsr*GI and *Bcl*I sites. The annealed oligonucleotides were ligated into the *Bsr*GI- and *Bcl*I-digested construction vector. To make double mutations, both N227D and N227E single mutants (Klassen et al., 2008) and jShak1 loop mutants were digested with *Cla*I and *Hpa*I restriction enzymes and the relevant fragments were recombined. Sequences of all the plasmids were confirmed by Sanger sequencing.

Mutants at single sites are named by the convention WT residue, position, mutant residue; for example, a mutant in which the asparagine residue at position 227 has been replaced by a glutamate residue is N227E. Replacements of the wild-type loop sequence (VSSSK) by other peptide sequences are designated by the new loop sequence in standard single-letter code; for example, the mutant with the wild-type loop replaced by 10 serines is S10, and that with the wild-type loop replaced by nine serines with a C-terminal lysine is S9K. Mutants made by replacing only the C-terminal lysine of the S3–S4 loop (K278) are designated as K278X mutants, where X can represent any amino acid; for example, K278A and K278G. Mutants with two mutations combined are designated as either ND or NE (representing N227E or N227E) followed by the loop mutation designation; for example, NDS10 is a mutant channel with a 10 serine (S10) synthetic loop and N227D mutation in the S2 helix (Table 1).

For expression in *Xenopus laevis* oocytes, plasmids were linearized by *Nde*I digestion, gel purified and the resulting DNA was used as a template to make mRNAs by *in vitro* transcription using a mMessage mMachine (Ambion, Austin, TX, USA) T7 polymerase kit. RNA was stored at −80°C until it was injected into oocytes.

Oocyte preparation

A lobe of ovary was surgically extracted from female *X. laevis* of 2–4 years of age and single oocytes were prepared and injected with synthesized mRNA as previously described (Sand et al., 2013). The protocols used for preparing oocytes from *X. laevis* were evaluated and approved by the Animal Care and Use Committee (Biosciences) of the University of Alberta (protocol AUP00000011).

Electrophysiology

Two-electrode voltage-clamp recording was performed 24–48 h after injection of mRNA using a GeneClamp 500B Amplifier, a Digidata 1322 A/D converter and pClamp9 software (Molecular Devices, Sunnyvale, CA, USA). Oocytes that had been injected with the different *in vitro* transcribed mRNA 1–3 days previously were subjected to a voltage protocol that held the cells at −90 mV before stepping to increasing voltages from −80 to +66 mV in 2 mV increments for a depolarization phase of 50 ms; then, the cells were repolarized to −50 mV for 50 ms. Current traces were filtered at 1 kHz and collected with P/4 leak subtraction. Recording was performed at room temperature with ND96 (96 mmol l^{-1} NaCl, 2 mmol l^{-1} KCl, 1.8 mmol l^{-1} $CaCl_2$, 1 mmol l^{-1} $MgCl_2$, 5 mmol l^{-1} Hepes-NaOH, pH 7.5) as the bath solution. jShak1 is sensitive to diisothiocyanatostilbene-2,2′-disulfonic acid (DIDS), which is often used to block endogenous chloride currents in *X. laevis* oocytes, so recordings were performed without DIDS in the bath solution. Uninjected oocytes from the same batch were evaluated and if there was significant endogenous current the mRNA-injected eggs were not used for measurement.

Data analysis

jShak1 is a very fast deactivating channel, with extremely fast tail currents. Recordings from non-injected eggs showed that the initial region of the tail current is corrupted by a transient that is only stabilized within 2 ms of the depolarizing pulse, making jShak1 tail currents unreliable for conductance–voltage analysis in our hands. However, in the ΔN23 channels, with the N-terminal inactivation domain removed, the outward current reaches a plateau after 50 ms of stimulation (Fig. 2, top panels); the steady-state outward current

Journal of Experimental Biology (2017) 220, 469-477 doi:10.1242/jeb.144089

Table 1. Description of channel mutations and the corresponding V_{50} values for all the channels used in this paper

Channel	Mutation sequence	V_{50} (mean±s.d.)	*N*
WT	VSSSK	33.0±3.3	14
N227D	Point mutation in S2 helix	17.7±3.7	5
N227E	Point mutation in S2 helix	−13.5±4.2	5
G3	GGG	60.4±1.5	7
G5	GGGGG	41.9±3.9	9
G4K	GGGGK	39.7±1.0	6
G10	GGGGGGGGGG	39.1±2.8	7
G9K	GGGGGGGGGK	36.4±7.5	7
E3	EEE	34.5±2.1	10
E5	EEEEE	32.1±1.9	7
E4K	EEEEK	34.4±3.6	4
S3	SSS	46.7±2.5	9
S5	SSSSS	40.9±3.7	11
S4K	SSSSK	34.0±1.7	6
S10	SSSSSSSSSS	30.3±4.0	10
S9K	SSSSSSSSK	30.6±2.7	4
K278A	VSSSA	37.0±3.8	8
K278G	VSSSG	24.1±8.5	6
K278S	VSSSS	27.2±3.8	7
K278N	VSSSN	34.8±6.6	7
K278Q	VSSSQ	33.6±3.0	9
K278D	VSSSD	17.7±3.5	9
K278E	VSSSE	21.2±6.8	6
NDG3	N227D+G3(GGG) loop	52.8±5.4	9
NDG5	N227D+G5 (GGGGG) loop	28.4±1.9	9
NDG4K	N227D+G4K (GGGGK) loop	29.3±3.4	9
NDG10	N227D+G10(GGGGGGGGGG) loop	26.1±3.0	9
NDG9K	N227D+G9K (GGGGGGGGGK) loop	30.5±1.5	7
NDE3	N227D+E3(EEE) loop	29.4±4.2	9
NDE5	N227D+E5 (EEEEE) loop	19.2±5.1	7
NDE4K	N227D+E4K (EEEEK) loop	26.3±5.1	6
NDS3	N227D+S3 (SSS) loop	31.0±2.3	6
NDS5	N227D+S5 (SSSSS) loop	27.8±5.8	7
NDS4K	N227D+S4K (SSSSK) loop	25.4±4.1	9
NDS10	N227D+S10 (SSSSSSSSSS) loop	14.6±2.8	6
NDS9K	N227D+S9K (SSSSSSSSSK) loop	20.5±3.8	9
NDK278A	N227D+K278A (VSSSA) loop	18.5±3.5	9
NDK278G	N227D+K278G (VSSSG)loop	8.9±5.1	9
NDK278S	N227D+K278S (VSSSS) loop	16.0±3.2	8
NDK278N	N227D+K278N (VSSSN) loop	22.4±2.2	9
NDK278Q	N227D+K278Q (VSSSQ) loop	16.0±2.6	9
NDK278D	N227D+K278D (VSSSD) loop	8.6±22.4	6
NDK278E	N227D+K278E (VSSSE) loop	16.9±4.7	7
NEG3	N227E+G3 (GGG) loop	10.6±2.7	4
NEG5	N227E+G5 (GGGGG) loop	−17.0±8.2	9
NEG4K	N227E+G4K(GGGGK) loop	1.9±3.3	9
NEG10	N227E+G10 (GGGGGGGGGG)loop	−17.2±4.0	4
NEE3	N227E+E3 (EEE) loop	−6.4±7.1	9
NEE5	N227E+E5(EEEEE) loop	−23.1±13.6	5
NEE4K	N227E+E4K (EEEEK) loop	−2.9±3.3	4
NES3	N227E+S3 (SSS) loop	−11.8±2.1	5
NES5	N227E+S5 (SSSSS) loop	−4.4±3.5	7
NES4K	N227E+S4K (SSSSK) loop	−6.9±1.8	6
NES10	N227E+S10 (SSSSSSSSSS) loop	−16.7±6.1	8
NES9K	N227E+S9K (SSSSSSSSSK) loop	−13.0±5.2	8
NEK278A	N227E+K278A (VSSSA) loop	−25.6±2.8	4
NEK278G	N227E+K278G (VSSSG) loop	−33.7±5.3	7
NEK278S	N227E+K278S (VSSSS) loop	−23.9±12.8	9
NEK278N	N227E+K278N (VSSSN) loop	−21.2±8.0	9
NEK278Q	N227E+K278Q (VSSSQ) loop	−19.4±10.2	8
NEK278D	N227E+K278D (VSSSD) loop	−46.1±8.8	9
NEK278E	N227E+K278E (VSSSE) loop	−31.6±16.6	9

is a linear function of voltage when the conductance has reached equilibrium. Although many of the mutant channels manifested slower kinetics than the wild-type channel shown in Fig. 2, the 50 ms depolarization step was long enough that the current traces all reached a plateau. Thus, we fitted the plateau currents (I) at each voltage step to the fourth order Boltzmann equation rearranged to represent current as a function of the clamp voltage (V):

$$I = \frac{G_{\max}(V - V_{\text{rev}})}{\left(1 + \exp\left(\frac{-(V - V_{50,\text{subunit}})}{b}\right)\right)^4}, \quad (1)$$

where $G_{\max}$ (maximum conductance for a given cell), $V_{50,\text{subunit}}$ (the holding potential at which 50% of individual subunits are in the activated state) and the slope factor, b, are the three fitted parameters. We chose the fourth order Boltzmann function for fitting (which yields V_{50} and slope values per subunit) because the opening of the ion channel is dependent on the activation of all four of the VSDs independently; we also compared first order and fourth order Boltzmann fits to the data and the fourth order fit consistently gave more precise fitting results (Fig. 2, bottom panels). The K^+ reversal potential (V_{rev}) was assumed to be a constant −70 mV for all channels (Yang et al., 1997). This choice was confirmed by inspection of the tail currents from the recordings, which revealed V_{rev} to be near −70 mV in all the recordings; small variations of this estimate of V_{rev} did not significantly change the values of the parameters inferred from the fittings.

Data fitting was performed using the fit function of MATLAB (release 2016a). Visual inspection of the fitted curves and the data indicated that when the adjusted R^2 value from the fittings was less than 0.998 there was an obvious mismatch of the fitted curve to the data, so recordings for further analysis were selected as having adjusted R^2 values greater than or equal to 0.998.

The V_{50} value for each tetrameric channel ($V_{50,\text{channel}}$), the voltage at which measured conductance (G) is half of the maximum conductance ($G_{\max}$), was calculated from the fitted $V_{50,\text{subunit}}$ from the fourth order fitting using the relationship:

$$\frac{G}{G_{\max}} = \frac{1}{2} = \frac{1}{\left(1 + \exp\left(\frac{-(V_{50,\text{channel}} - V_{50,\text{subunit}})}{b}\right)\right)^4}, \quad (2)$$

yielding the equation:

$$V_{50,\text{channel}} = V_{50,\text{subunit}} - b \times \ln(\sqrt[4]{2} - 1). \quad (3)$$

Statistical treatment

Statistical significance of differences between V_{50} values of the different mutant channels was evaluated by determining mean and standard deviation of replicate measurements (see Table 1) and comparing pairwise combinations using unpaired *t*-tests as implemented in the R statistical suite of programs (https://www.r-project.org/) (Table S1). Comparisons using the non-parametric Kruskal–Wallis test as modified by Conover and Iman (1976) were also performed; we found that the *t*-test was more conservative, in that in a few cases of marginal differences the *P*-value from the *t*-test was >0.05 when the non-parametric test gave a *P*-value that was <0.05, so we have used the *t*-test throughout this paper.

Box-and-whisker plots for figures comparing the measurements were prepared using the Lattice package (Sarkar, 2008) in the R statistical suite.

Journal of Experimental Biology (2017) 220, 469-477 doi:10.1242/jeb.144089

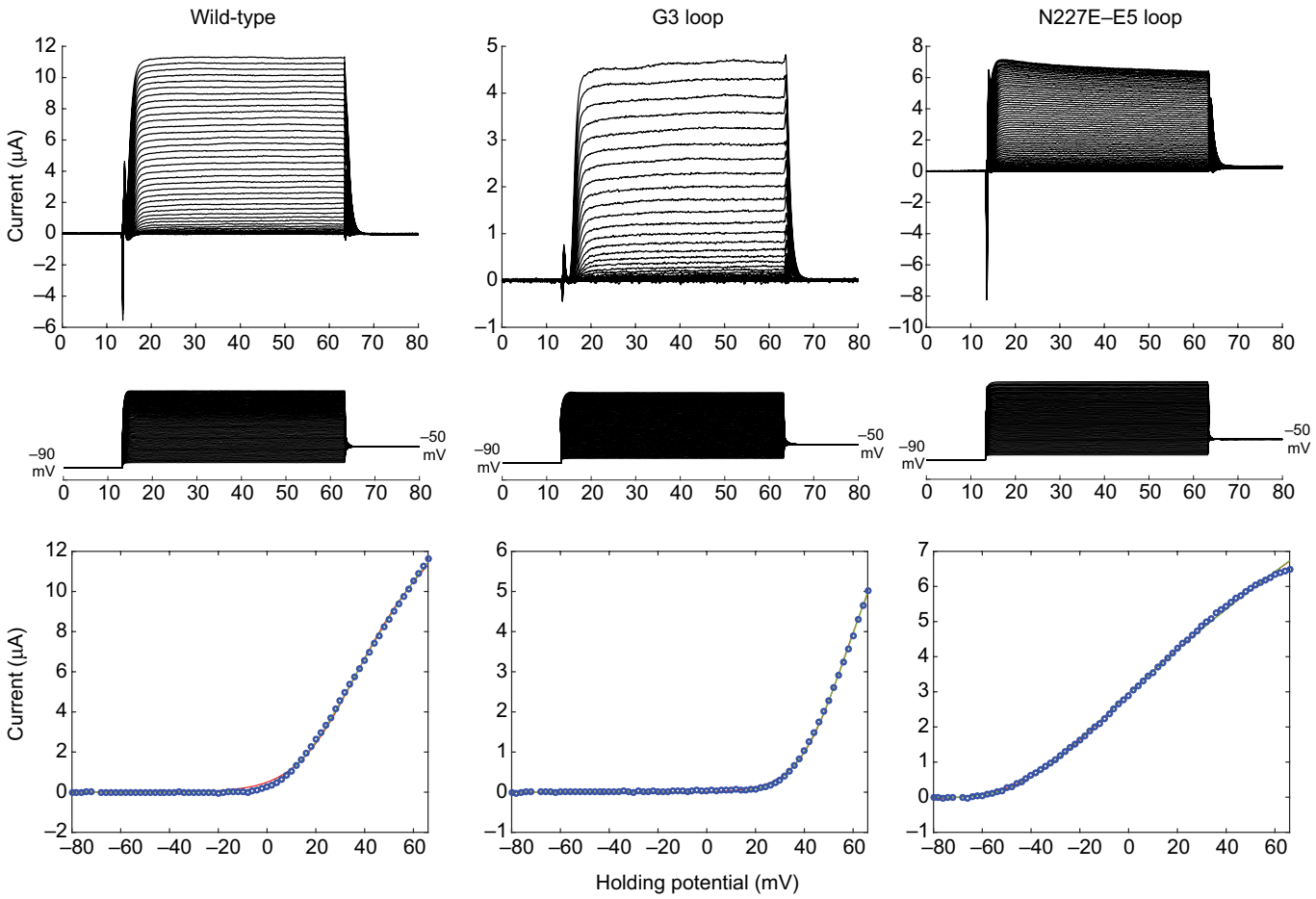

Fig. 2. Example voltage-clamp trace data from wild-type and mutant Δ23-jShak1 channels, expressed in *Xenopus laevis* oocytes. (Left) Wild-type; (center) the most positively shifted mutant, with a G3 loop replacement mutation; and (right) one of the most negatively shifted mutants, a combination of the N227E and E5 loop mutations. The top panels represent current traces from an oocyte expressing the channel, which was held at –90 mV and then depolarized in 2 mV increments to voltages from –80 to +66 mV for 50 ms. Channels reach a plateau current that is stable to the end of the 50 ms stimulation voltage. The middle panels show the corresponding voltage traces. The bottom panels show plateau current values at each of the 2 mV depolarization steps as a function of the step voltage (blue open circles) from –80 to +66 mV and the fitted curves for the first order (red) and fourth order (green) Boltzmann equations. The fourth order equation consistently gave better fitting over the range of voltages tested and was used to derive the parameters as described in Materials and methods.

Molecular modeling

An open-state homology model of jShak1 was created in SWISS MODEL using 3LUT (the enhanced crystal structure of rat Kv1.2; Chen et al., 2010) as a template. A similar approach was taken to model the closed state of jShak1, using an inferred closed-state model of the Kv1.2/Kv2.1 'paddle chimera' (Long et al., 2007) from Jensen et al. (2012) as a template. Selected parts of these homology models were used in constructing figures, using PyMol (version 1.8.4, https://www.pymol.org/). These illustrations are included as heuristic aids for interpreting the experimental results.

Results

In the present study, the natural five-residue (VSSSK) S3–S4 linker of jShak1 (Fig. 1, yellow and orange residues, atoms rendered as spheres) was replaced with synthetic homopolymers varying in length and composition. The C-terminal residue of the loop, K278 (Fig. 1, orange residue), was also mutated in both natural and synthetic loops. To evaluate the effect of the loop length and composition on the interactions within the VSD, mutations of the neutral asparagine (N) at position 227 of jShak1 (Fig. 1, dark blue residue, atoms rendered as spheres) to either glutamate (E) or aspartate (D) were combined with all synthetic loops to make double-mutant channels. The remainder of the channel is rendered in green in cartoon format (https://www.pymol.org/).

Effects of length and composition of homopolymeric S3–S4 loops on jShak1

The V_{50} values of the G3 (+60.4 mV), G5 (+41.9 mV) and G10 (+39.1 mV) loop mutants (Fig. 3) illustrate that simply changing the identity of the residues in the S3–S4 loop and the length of the loop can significantly affect voltage sensitivity. The shorter the loop, the more positively shifted the V_{50} value from the wild-type value, and therefore the more stable the closed state relative to the open state of the channel. As the loop was lengthened, the V_{50} value for the channel approached a value closer to, but still more positive than, the value for the wild-type channel (P=0.031 for the G10 loop compared with the WT loop).

Similarly, the V_{50} of the S3 loop replacement mutant in jShak1 (+46.7 mV) was significantly more positive than that of the wild-type channel (P=2.2×10^{-7}). The longer serine loops (S5, V_{50}= +40.9 mV and S10, V_{50}=+30.3 mV) shifted the V_{50} to more negative values compared with that for the S3 loop, and converged on the V_{50} of the wild-type channel (P=0.30 for comparison of wild-

Journal of Experimental Biology (2017) 220, 469-477 doi:10.1242/jeb.144089

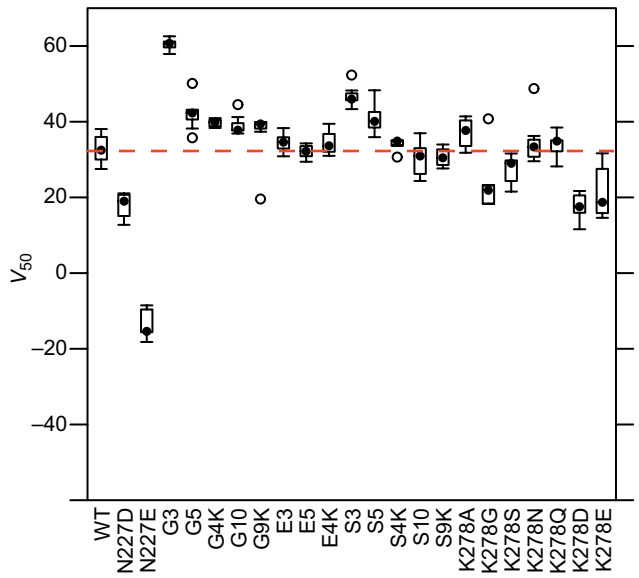

Fig. 3. Voltage of half activation (V_{50}) of jShak1 with single mutations, N227D or N227E mutations or different S3–S4 loops replacing the wild-type loop. The box-and-whisker plots (Sarkar, 2008) indicate the median value of multiple measurements as a black dot, with the box indicating the range from first to third quartile and open circles indicating outlier measurements. Means and standard deviations for these data are presented in Table 1. The horizontal red dashed line is drawn at the median V_{50} value of the wild-type (WT) channel to clarify the comparison of the different box-and-whisker ranges.

type and S10 channel) (Fig. 3). This is not surprising as the native loop sequence is VSSSK.

The V_{50} values of E3 and E5 were not significantly different from the wild-type jShak1 V_{50} (P=0.59 and 0.75, respectively). Both E3 and E5 are more negative than the other mutant loops with neutral (G and S) amino acids of the same length (Fig. 3). The E10 homopolymer loop in jShak1 did not produce a functional channel.

These results illustrate two general principles: (1) the length of the S3–S4 loop can have significant effects on the voltage sensitivity of the channel, and (2) the composition of the loops also has a significant effect, i.e. the loops do not simply act as passive tethers constraining the movement of the S3 and S4 helices. In particular, short loops always bias the channel V_{50} to more positive values, indicating substantial stabilization of the closed state or destabilization of the open state.

Effects of mutation of the C-terminal residue of the S3–S4 loop

In the mouse Kv1.2 channel, the C-terminal region of the S3–S4 linker is proposed to be pulled downward on channel deactivation and the VSD rotates towards the PD, bringing the C-terminal end of the S3–S4 loop closer to the negatively charged residues of the VSD and the PD turret in the closed state (Jensen et al., 2012); mutations of this C-terminal region significantly affect the V_{50} of mouse Kv1.2 (Sand et al., 2013). We mutated the C-terminal residue of the S3–S4 loop of jShak1 in both natural and synthetic loops to evaluate the effect of the C-terminal residue of the S3–S4 linker on the V_{50} values of jShak1.

The negatively charged residues (D, E) at the C-terminus of the wild-type loop significantly shifted the V_{50} to approximately 10 mV less positive values (V_{50}=+17.7 mV, P=8.3×10^{-9} and V_{50}=+21.2 mV, P=8.2×10^{-5} for K278D and K278E, respectively). The K278G (V_{50}=+24.1 mV, P=0.0028) and K278S (V_{50}=+27.2 mV, P=0.04) mutations also caused small but statistically significant negative shifts in V_{50} (Fig. 3). The changes in the V_{50} values for K278A (V_{50}=+37.0 mV, P=0.14), K278N (V_{50}=+34.8 mV, P=0.52) and K278Q (V_{50}=+33.6 mV, P=0.81) were not statistically significant (Fig. 3).

We also replaced the C-terminal residue of the homopolymer loops of the same length as the wild-type loop with lysine (K), the natural residue at the C-terminus of the jShak1 S3–S4 linker. G5 and G4K V_{50} values did not differ (P=0.50), but the difference between S5 and S4K V_{50} values, 6.9 mV, was statistically significant (P=0.027), and the S4K value (V_{50}=+34 mV) did not differ from the wild-type (VSSSK) loop sequence V_{50} (P=0.73). The E4K V_{50} did not differ significantly from that of the wild-type channel (P=0.68) or from the V_{50} value of the E5 channel (P=0.55).

A similar comparison of the V_{50} values for the 10-residue loops showed that G10 and G9K V_{50} values did not differ significantly (P=0.40), and S10 and S9K V_{50} values did not differ (P=0.93). Long glutamate loops did not produce detectable channel activity.

Double mutations of the S3–S4 loop and residue 227 in the S2 helix functionally interact in jShak1

One of the residues of the S2 helix that is acidic in almost all other homologous channels (E283 in *D. melanogaster* and E226 in mouse Kv1.2) and stabilizes the open state by forming a salt bridge with a basic residue in the S4 helix is replaced by neutral asparagine, N227, in jShak1. Previous mutagenesis studies with jShak1 (Klassen et al., 2008) have shown that both N227D and N227E mutations stabilize the open state, with a substantial negative shift in the V_{50} value. The N227E mutation caused a greater negative shift than the N227D mutation, presumably because the longer glutamate side-chain allows the negatively charged carboxyl group closer access to the positively charged residues in S4 than the shorter aspartate side-chain (Klassen et al., 2008). However, the N227E mutation appeared to have steric clashes with other parts of the VSD when the S4 helix was lengthened that were not found in the N227D mutants, indicating that the short natural S3–S4 loop of jShak1 imposes a constraint on the helices within the VSD that leads to tight restrictions on the relative positions of helices in the VSD. We made double-mutant channels by combining the N227D and N227E mutations with the loop mutations described above, to evaluate the effects of S3–S4 loop length and composition on the N227 mutant channels.

Both N227D (V_{50}=+17.7 mV, P=2.1×10^{-6}) and N227E (V_{50}=−13.5 mV, P=3×10^{-39}) single mutants (Fig. 3) stabilized the open state compared with the wild-type channel, N227E being more effective than N227D (P=6.7×10^{-15}), as previously reported (Klassen et al., 2008). In N227D and N227E mutants, the negatively charged residue in the S2 helix appears to form a salt bridge with the positively charged residues of the S4 helix (Klassen et al., 2008), as is the case in the *D. melanogaster* Shaker channel (Papazian et al., 1995; Seoh et al., 1996) and the mouse Kv1.1 channel (Planells-Cases et al., 1995).

Combining the G3 loop with N227D and N227E mutations (Figs 4 and 5) yielded a large relative stabilization of the open state compared with the single N227D and N227E mutations, as is seen in the wild-type background; NDG3 and NEG3 channels had a much more positive V_{50} than N227D (35.1 mV, P=2.5×10^{-22}) and N227E (24.1 mV, P=8.4×10^{-9}), respectively.

The longer glycine loops had the same effect on the N227D and N227E channel behavior as they did in the wild-type context, producing V_{50} values that were closer to, but more positive than, the values for the N227D/E mutants. NDG5 V_{50} (+28.4 mV) and

Journal of Experimental Biology (2017) 220, 469-477 doi:10.1242/jeb.144089

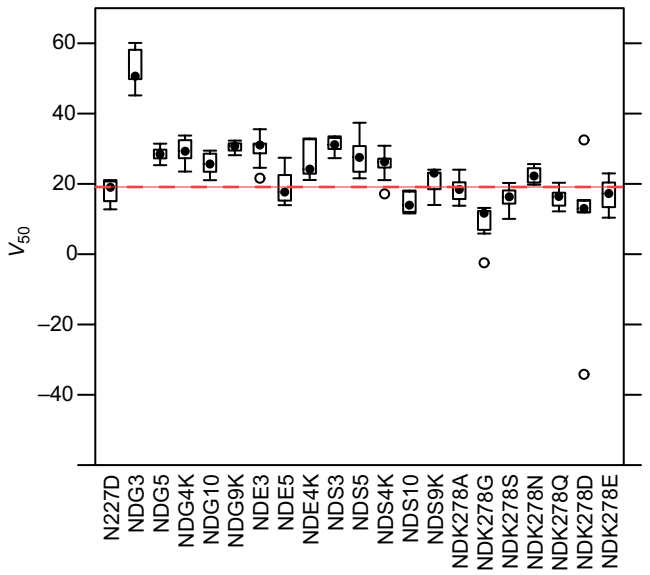

Fig. 4. V_{50} of jShak1 double mutations with different S3–S4 loops replacing the wild-type loop in combination with the N227D mutation in the S2 helix. Details as in Fig. 3. Means and standard deviations for these data are presented in Table 1. The horizontal red dashed line is drawn at the median V_{50} value of the N227D channel to clarify the comparison of the different box-and-whisker ranges.

NDG10 V_{50} (+26.1 mV) were not significantly different from each other (P=0.42), and were substantially closer to, but still significantly more positive than, N227D V_{50} (P=0.0017 and P=0.014, respectively) (Fig. 4). In contrast, the NEG5 and NEG10 channels had V_{50} values that were no different from that of the N227E channel (V_{50}=−17 mV, P=0.29 and V_{50}=−17.2 mV, P=0.36, respectively) (Fig. 5).

The replacement of the C-terminal residue of the glycine loops with a lysine residue in the double mutations with N227D caused no

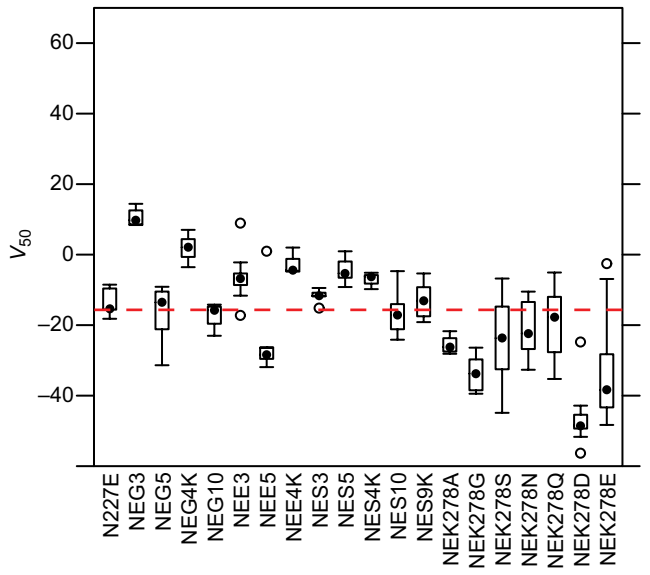

Fig. 5. V_{50} of jShak1 double mutations with different S3–S4 loops replacing the wild-type loop in combination with the N227E mutation in the S2 helix. Details as in Fig. 3. Means and standard deviations for these data are presented in Table 1. The horizontal red dashed line is drawn at the median V_{50} value of the N227E channel to clarify the comparison of the different box-and-whisker ranges.

significant change in V_{50} from that for the homopolymeric loop of the same length (Fig. 4). The V_{50} (+1.9 mV) of NEG4K, in contrast, was significantly more positive (by approximately 19 mV) than that of NEG5 (P=1.3×10^{-10}) and N227E (P=8.1×10^{-6}) (Fig. 5), indicating that the additional constraint of the longer glutamate side-chain at position 227 causes a significant, indirect interaction with the C-terminal lysine on the G4K loop that is absent in the N227D mutation, and that stabilizes the closed state of the channel. The NEG9K channel did not express a detectable current.

Thus, the presence of the longer acidic side-chain with glutamate as opposed to aspartate at position 227 has a substantially different effect on the interaction between the loop's C-terminal lysine and the rest of the channel.

Combining the N227D mutation and serine S3–S4 loops had qualitatively similar effects to introduction of the loop mutations in a wild-type background (Fig. 4). For the wild-type and N227D combinations, the S3 chain differed significantly from the corresponding wild-type loop (P=2.2×10^{-7} for wild-type, P=3.5×10^{-4} for N227D), as did the S5 chain (P=0.0014 for wild-type, P=0.0048 for N227D), but the S10 loop had the same effect as the wild-type loop (P=0.29 for wild-type, P=0.39 for N227D). In contrast, in the context of the N227E mutation, the S3 and S10 loops had no significant effect compared with the N227E mutation alone (P=0.66 and P=0.35, respectively) while the S5 loop did have a small effect, increasing V_{50} by approximately 9 mV (P=0.01) (Fig. 5). The S9K mutation in both N227D and N227E backgrounds yielded V_{50} values no different from the N227D and N227E single mutants, respectively (P=0.42 and P=0.90, respectively), but the S4K loop, which had no significant effect in the wild-type (P=0.73) or N227E background (P=0.076), did yield a positive shift in V_{50} of approximately 8 mV in the N227D background (P=0.024).

The E3 and E4K loops, which did not show a significant difference in V_{50} from each other in the wild-type background, did cause a significant positive shift in V_{50} in the context of the N227D mutation (Fig. 4) (11.7 mV, P=6.3×10^{-4} for NDE3 and 8.6 mV, P=0.02 for NDE4K), whereas the NDE5 V_{50} value was not significantly different from that of the N227D channel (P=0.67). In the context of the N227E mutation, the E3 mutation moved the V_{50} approximately 7 mV more positive (P=0.037) than a channel with a single N227E mutation, the E5 mutation shifted the V_{50} approximately 10 mV more negative (P=0.013) and the E4K loop mutation shifted the V_{50} value more positive by approximately 10 mV (P=0.01) (Fig. 5).

To further evaluate how mutations of the C-terminal residue of the S3–S4 loop in jShak1 interact with the residue at position 227, we combined the K278 mutations with the N227D and N227E mutations. The K278A, K278N and K278Q mutations had no significant effect on the wild-type and N227D channel V_{50} values. The K278G mutation caused a significant negative shift in V_{50} in wild-type and N227D backgrounds (ΔV_{50}=8.9 mV, P=0.0028 and ΔV_{50}=8.8 mV, P=0.0095, respectively). K278S, K278D and K278E mutations caused channel V_{50} to shift to more negative values (ΔV_{50}=5.8 mV, P=0.04, ΔV_{50}=15.3 mV, P=8.3×10^{-9} and ΔV=11.8 V, P=8.2×10^{-5}, respectively) in the wild-type but not in the N227D background. In the N227E background, all of the K278 mutations except K278Q yielded significantly more negative V_{50} values than the N227E mutation alone.

DISCUSSION

The structural basis for quantitative differences in voltage sensitivity is a complex problem. Interaction networks between transmembrane helices within the VSD contribute to relative

Journal of Experimental Biology

Journal of Experimental Biology (2017) 220, 469-477 doi:10.1242/jeb.144089

stabilization of the open and closed states of the channel (Lee et al., 2005; Long et al., 2005; Papazian et al., 1995). The S3–S4 loop, varying in both length and composition within and between different families of Kv channels, also affects V_{50} significantly (Gonzalez et al., 2000, 2001; Labro et al., 2015; Priest et al., 2013; Sand et al., 2013).

During the evolution of the Kv channel families, all parts of the channel protein have undergone changes to some extent, and these accumulated changes are the context in which subsequent new mutations affect channel behavior. To get a broad insight into how the sequence of Kv channels affects their voltage sensitivity, it is necessary to investigate the effects of synthetic mutations in the context of evolutionarily divergent channels. This approach can illuminate general principles of channel activation and identify how those general principles are modulated by changes in specific sequence elements.

In this study, we have evaluated the effects of mutations in two parts of a Kv1 family channel that have been demonstrated to play significant roles in setting voltage sensitivity, in the context of a cnidarian channel that is highly diverged from the bilaterian channels in which most previous studies have been performed.

Effects of S3–S4 loop mutations

The natural S3–S4 loop of jShak1 (VSSSK) was replaced with synthetic homopolymeric loops varying in length (3, 5 and 10 amino acids) and composition (glycine, serine, glutamic acid). Loops of three residues of neutral amino acids biased the channel towards the closed-state conformation (V_{50} was more positive than wild-type) and as the loop length increased, the V_{50} values asymptotically approached a more negative value, indicating increasing stability of the open state relative to the closed state. This indicates that the physical constraint imposed on the distance between the C-terminal end of the S3 helix and the *N*-terminal end of the S4 helix by the loop connecting them can be a significant factor in setting the V_{50} of the channel, especially at short loop lengths. The fact that the glycine loop series and the serine loop series reached different V_{50} values as the loops lengthened indicates that the composition of the loop is also a factor, presumably by virtue of direct non-covalent interaction with other parts of the channel protein. This direct non-covalent interaction of the loop is more apparent in the case of the glutamate loop mutants. The E3 and E5 loop mutations in the wild-type background had the same V_{50} values as the wild-type channel, indicating that the charged loop residues stabilize the open state (relative to the closed state) against the effect of the extremely short loop, which would be expected to do the opposite. These results imply that there is a strong electrostatic interaction between the loop and other parts of the channel protein that stabilizes the open state sufficiently to overcome the closed-state stabilization expected from very short loops.

Identical synthetic mutations affect V_{50} differently in mouse Kv1.2 (Sand et al., 2013). In Kv1.2, long glycine and serine loops both converge on the same V_{50} value as the wild-type loop, while the glutamate loops converge on a V_{50} value that is ∼14 mV more negative than that of the wild-type channel.

Effects of combinations of S3–S4 loop mutations and N227 mutations

One of the atypical aspects of the jShak1 channel is the presence of an asparagine at position 227, whereas almost all other Kv1 channels have a glutamate residue at the homologous position. This amino acid difference is a major factor in the unusually positive V_{50} value of the jShak1 channel, as mutating it to a glutamate residue creates a channel with a more typically negative V_{50}. Combining N227D or N227E mutations with the loop mutations clearly demonstrates that there is a functional interaction (although not necessarily a direct physical interaction) between these two characters. The effects of the different loop sequences in the context of the three different amino acid residues are illustrated directly in Fig. 6. If the two elements, loop sequence and amino acid at position 227, were acting independently, then the effect of a

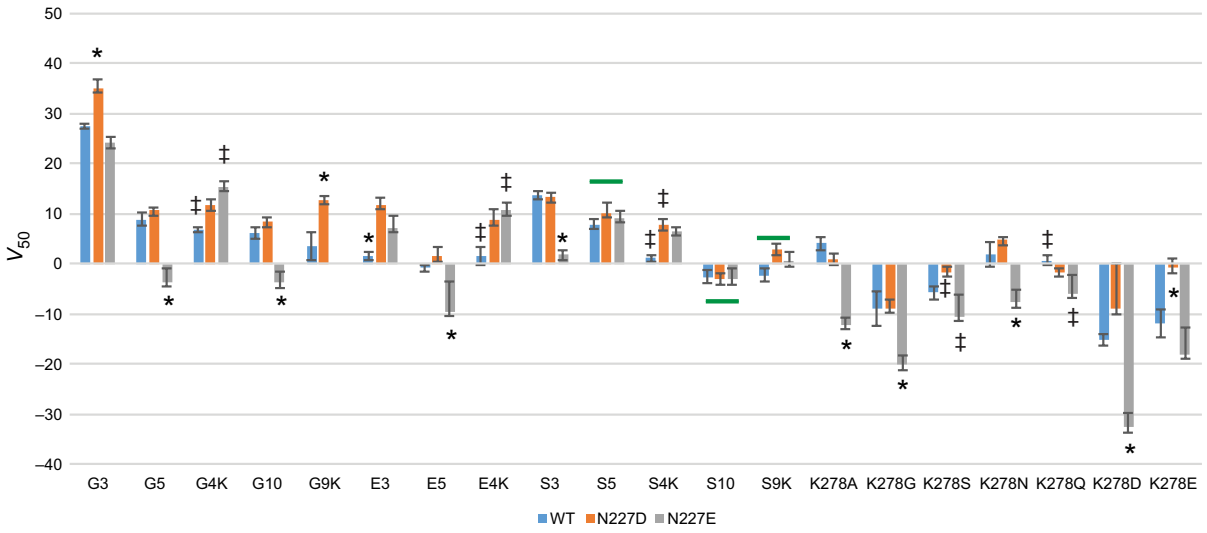

Fig. 6. Comparison of the effects of the various loop mutations in the context of asparagine (WT), aspartate (N227D) and glutamate (N227E) at position 227 of the jShak1 channel. The bars (±s.e.m.) represent the difference in V_{50} value between the channel with the wild-type S3–S4 loop and the channel with the mutant loop in the context of the three different residues at position 227. Negative values indicate that the loop stabilizes the open state more than the closed state in the context of the specific residue at position 227 and positive values indicate that the closed state is preferentially stabilized compared with the open state. Three sets of symbols are used to annotate the significance of differences within each loop variant: (1) an asterisk marks a value that is significantly different from the other two values, which in turn are not significantly different from each other, (2) double daggers mark two values that are significantly different from each other but not different from the third value, and (3) a green bar marks sets of three values among which there is no significant difference.

Journal of Experimental Biology (2017) 220, 469-477 doi:10.1242/jeb.144089

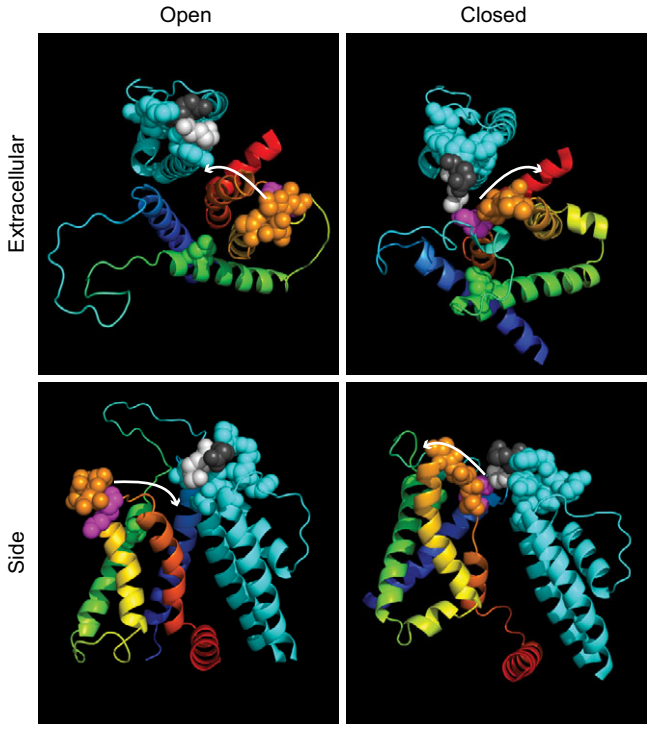

Fig. 7. Illustration of movement and interactions of the S3–S4 linker in the open and closed states of Kv channels. The four helices and connecting loops of a single voltage-sensing domain (VSD) are represented in cartoon format, to illustrate the overall structure, with a color scheme that progresses from blue at the N-terminus of the fragment shown through green, yellow and orange to red at the C-terminus of the fragment shown. The pore region of the adjacent subunit in the channel tetramer, which interacts most closely with the VSD, is shown in cyan. Orthogonal views are shown from the extracellular aspect and a lateral aspect selected to make the relationships between the helices as clear as possible. Open and closed states were aligned using only the relatively immobile pore structure to illustrate the relative movements of the parts of the VSD. Atoms of the side-chain of residue N227 are shown as green spheres, those of the VSSS sequence of the loop as orange spheres, those of K278 as magenta spheres, those of the pore vestibule loop as cyan spheres, and those of the adjacent lysine and glutamate residues of the vestibule loop that are closest to the VSD as light gray and dark gray spheres, respectively. The white arrows indicate the direction of movement and rotation of residue K278 in the transition from the open to closed and closed to open state.

changed loop would be the same in all three of the N227, N227D and N227E backgrounds. This is not the case in general.

The V_{50} values for channels combining N227E and the G5 and G10 loops were significantly shifted to a more negative value than would be expected from the combinations of the same loops with N227 or N227D, but this effect was absent when the C-terminal residue of the loop was replaced with lysine. In contrast, the serine loops appeared to have comparable effects in the presence of any of the three residues at position 227, with or without the C-terminal substitution of lysine in the loop. In channels combining the E3, E5 and E4K loops with N227, the negative charge of the loops seemed to offset any effects of the short loop length; none of these three channels differed significantly from the wild-type channel in terms of V_{50}. In the presence of the N227D and N227E mutations, the E3 loops tended to stabilize the closed state relative to the open state; this effect disappeared (for N227D) or was reversed (for N227E) when the E5 loop was present, but the presence of a lysine at the C-terminal position of the E4K loop stabilized the closed state relative to the open state in the presence of both N227D and N227E.

Comparison of the effects of the point mutations at position K278 in the context of the three different residues at position 227 suggested a significant role for this residue in the interactions that affect voltage sensitivity. Replacement of K278 with either neutral (A, G) or polar (S, N, Q) residues had a minimal effect in the context of the wild-type N227 or the mutant N227D, but the open state was strongly stabilized relative to the closed state in the context of N227E.

Fig. 7 illustrates the relative positions of the S3–S4 loop (including position 278) and residue 227 within the structural framework of a single VSD and the adjacent pore region with which it physically interacts, in homology models of the open and closed states. In the closed state, the S3–S4 loop is drawn down into the VSD, which rotates away from the adjacent pore region. As a result, the loop, especially the C-terminal residue, is in much closer proximity to the residue at position 227 in the closed state than in the open state, and the rest of the loop is brought into proximity of residues in the flexible vestibule of the pore region.

These results from jShak1, when considered in the context of comparable studies in phylogenetically diverse homologues, indicate that the loop sequence interacts with the rest of the channel as well as being a tether restricting the dynamics of the S4 helix. The S3–S4 loop in jShak1 affects the V_{50} in the following ways. (1) Very short neutral S3–S4 loops constrain the transition of the S4 helix across the membrane and its interaction with the S2 helix in the closed-to-open transition, thus yielding a relatively positive V_{50} value, whereas the E3 loop has little effect on V_{50} in the context of the N227 (wild-type at position 227) channel. (2) Converting the asparagine at position 227 to an acidic aspartate or glutamate residue robustly stabilizes the open state by forming a salt bridge with the arginine residues in the S4 helix, but short neutral loops act against this stabilization, arguably by forcing the arginine and acidic residues into steric clashes with a substantial repulsive force. (3) The C-terminus of the S3–S4 loop has significant effects largely on channels that also have glutamate at position 227 (N227E), in that smaller and neutral side-chains show a negative shift in V_{50} that is not observed in the case of the wild-type N227 and N227D mutant channels. This may be due to the fact that the C-terminal lysine residue of the loop can interact more strongly with a glutamate side-chain at position 227 in the closed state because the longer side-chain of the glutamate at position 227 (N227E) allows closer apposition of the acidic and basic residues than is the case for aspartate (N227D), and in the wild-type channel the N227 residue is neutral and therefore does not mediate a strong electrostatic attraction with the positively charged lysine residue.

The wide diversity of Kv channel behaviors has arisen over the course of evolution by fixation of mutations that confer novel and, at the time, advantageous properties on these proteins. We previously reported on the effect of a variety of mutations in the S3–S4 loop of the mouse Kv1.2 channel (Sand et al., 2013). Those results illustrated that both the length and composition of this loop affect the response of the channel to changes in transmembrane voltage.

Degeneracy and non-additivity of effects of double mutations

The results of the present study illustrate that identical loop mutations in a different Kv1 homolog have quantitatively different effects, illustrating that the context of the loop mutation determines how its changed sequence affects the energetics of the conformational transitions that lead to channel opening and closing. By combining these loop mutations with changes to the N227 amino acid residue in jShak1, we also demonstrate that the effect of loop mutations is sensitive to changes in the collateral

interactions between the S2 and S4 helices that are at the core of the VSD (Fig. 7).

The large number of mutant channels that we tested also demonstrates that although single mutations will often cause large changes in the V_{50} of channel opening (for example, the large changes caused by the mutations of N227), those same mutations, when combined with mutations at other locations, can yield a set of channels with small differences in V_{50}. We also found that many different combinations of mutations of a single parental channel can lead to similar voltage sensitivity; for example, the N227D–S3 combination produced a channel with nearly the same V_{50} value as the E5 loop mutation alone and the unmutated channel (+31 to +33 mV), although the V_{50} for N227D was +17.7 mV and the V_{50} for S3 was +46.7 mV. Conversely, the combination of N227D–K278D yielded a channel with V_{50}=+8.6 mV, nearly identical to the V_{50} values for N227D alone or K278D alone, indicating that the effects of these two mutations are not additive.

Acknowledgements
The authors wish to thank Matthias Ostermaier who constructed a number of the mutant channels described in this paper during a research internship funded by University of Alberta International through the University of Alberta Research Experience program.

Competing interests
The authors declare no competing or financial interests.

Author contributions
N.S. and W.J.G. both contributed to experimental design and planning. N.S. (with contribution from Matthias Ostermaier, see above) constructed the mutant plasmids and performed the electrophysiological measurements. N.S. and W.J.G. both contributed to data analysis and writing this report.

Funding
This research was supported by the Natural Sciences and Engineering Research Council of Canada [Discovery Grant NSERC RGPIN 36402 to W.J.G.].

Supplementary information
Supplementary information available online at
http://jeb.biologists.org/lookup/doi/10.1242/jeb.144089.supplemental

References
Chen, X., Wang, Q., Ni, F. and Ma, J. (2010). Structure of the full-length Shaker potassium channel Kv1.2 by normal-mode-based X-ray crystallographic refinement. *Proc. Natl. Acad. Sci. USA* **107**, 11352-11357.
Conover, W. J. and Iman, R. L. (1976). On some alternative procedures using ranks for the analysis of experimental designs. *Commun. Stat. Theory Methods* **5**, 1349-1368.
Durell, S. R., Shrivastava, I. H. and Guy, H. R. (2004). Models of the structure and voltage-gating mechanism of the shaker K+ channel. *Biophys. J.* **87**, 2116-2130.
Gonzalez, C., Rosenman, E., Bezanilla, F., Alvarez, O. and Latorre, R. (2000). Modulation of the Shaker K(+) channel gating kinetics by the S3–S4 linker. *J. Gen. Physiol.* **115**, 193-208.
Gonzalez, C., Rosenman, E., Bezanilla, F., Alvarez, O. and Latorre, R. (2001). Periodic perturbations in Shaker K+ channel gating kinetics by deletions in the S3-S4 linker. *Proc. Natl. Acad. Sci. USA* **98**, 9617-9623.
Grigoriev, N. G., Spafford, J. D., Gallin, W. J. and Spencer, A. N. (1997). Voltage sensing in jellyfish Shaker K+ channels. *J. Exp. Biol.* **200**, 2919-2926.
Ho, S. N., Hunt, H. D., Horton, R. M., Pullen, J. K. and Pease, L. R. (1989). Site-directed mutagenesis by overlap extension using the polymerase chain reaction. *Gene* **77**, 51-59.
Jensen, M. O., Jogini, V., Borhani, D. W., Leffler, A. E., Dror, R. O. and Shaw, D. E. (2012). Mechanism of voltage gating in potassium channels. *Science* **336**, 229-233.
Klassen, T. L., O'Mara, M. L., Redstone, M., Spencer, A. N. and Gallin, W. J. (2008). Non-linear intramolecular interactions and voltage sensitivity of a KV1 family potassium channel from Polyorchis penicillatus (Eschscholtz 1829). *J. Exp. Biol.* **211**, 3442-3453.
Labro, A. J., Priest, M. F., Lacroix, J. J., Snyders, D. J. and Bezanilla, F. (2015). Kv3.1 uses a timely resurgent K(+) current to secure action potential repolarization. *Nat. Commun.* **6**, 10173.
Lee, S.-Y., Lee, A., Chen, J. and MacKinnon, R. (2005). Structure of the KvAP voltage-dependent K+ channel and its dependence on the lipid membrane. *Proc. Natl. Acad. Sci. USA* **102**, 15441-15446.
Li-Smerin, Y., Hackos, D. H. and Swartz, K. J. (2000). alpha-helical structural elements within the voltage-sensing domains of a K(+) channel. *J. Gen. Physiol.* **115**, 33-50.
Long, S. B., Campbell, E. B. and MacKinnon, R. (2005). Voltage sensor of Kv1.2: structural basis of electromechanical coupling. *Science* **309**, 903-908.
Long, S. B., Tao, X., Campbell, E. B. and MacKinnon, R. (2007). Atomic structure of a voltage-dependent K(+) channel in a lipid membrane-like environment. *Nature* **450**, 376-382.
Papazian, D. M., Shao, X. M., Seoh, S.-A., Mock, A. F., Huang, Y. and Wainstock, D. H. (1995). Electrostatic interactions of S4 voltage sensor in Shaker K+ channel. *Neuron* **14**, 1293-1301.
Planells-Cases, R., Ferrer-Montiel, A. V., Patten, C. D. and Montal, M. (1995). Mutation of conserved negatively charged residues in the S2 and S3 transmembrane segments of a mammalian K+ channel selectively modulates channel gating. *Proc. Natl. Acad. Sci. USA* **92**, 9422-9426.
Priest, M. F., Lacroix, J. J., Villalba-Galea, C. A. and Bezanilla, F. (2013). S3-S4 linker length modulates the relaxed state of a voltage-gated potassium channel. *Biophys. J.* **105**, 2312-2322.
Sand, R., Sharmin, N., Morgan, C. and Gallin, W. J. (2013). Fine-tuning of voltage sensitivity of the Kv1.2 Potassium channel by inter-helix loop dynamics. *J. Biol. Chem.* **288**, 9686-9695.
Sarkar, D. (2008). *Lattice: Multivariate Data Visualization with R*, 265 pp. New York: Springer.
Seoh, S.-A., Sigg, D., Papazian, D. M. and Bezanilla, F. (1996). Voltage-sensing residues in the S2 and S4 segments of the Shaker K+ channel. *Neuron* **16**, 1159-1167.
Silverman, W. R., Roux, B. and Papazian, D. M. (2003). Structural basis of two-stage voltage-dependent activation in K+ channels. *Proc. Natl. Acad. Sci. USA* **100**, 2935-2940.
Team, R. C. (2015). *R: A Language and Environment for Statistical Computing*. Vienna, Austria: R Foundation for Statistical Computing.
Tiwari-Woodruff, S. K., Schulteis, C. T., Mock, A. F. and Papazian, D. M. (1997). Electrostatic interactions between transmembrane segments mediate folding of Shaker K+ channel subunits. *Biophys. J.* **72**, 1489-1500.
Tombola, F., Pathak, M. M. and Isacoff, E. Y. (2006). How does voltage open an ion channel? *Annu. Rev. Cell Dev. Biol.* **22**, 23-52.
Yang, Y., Yan, Y. and Sigworth, F. J. (1997). How does the W434F mutation block current in Shaker potassium channels? *J. Gen. Physiol.* **109**, 779-789.

Table S1

Click here to Download Table S1